Yearly Report: May 2007

Methane Recovery from Hydrate-bearing Sediments

Funding Number: DE-FC26-06NT42963

Submitted By:

J. Carlos Santamarina
Georgia Institute of Technology
School of Civil and Environmental Engineering
Atlanta, GA 30332-0355
Phone: (404)-894.7605
Fax: (404)-894.2278
E-mail: jcs@gatech.edu

Costas Tsouris
Oak Ridge National Laboratory
Georgia Institute of Technology
School of Civil and Environmental Engineering
Atlanta, GA 30332-0373
E-mail: costas.tsouris@ce.gatech.edu

INTRODUCTION - PROJECT SUMMARY - STATUS

Gas hydrates constitute an attractive source of energy. It is estimated that one volume of natural gas hydrate has a methane content equivalent to 164 volumes of gaseous methane obtained from normal gas reservoirs. However, the development of technically and economically feasible methane production strategies from gas hydrate reservoirs is hindered by the many gaps in our understanding of gas hydrates.

Understanding and modeling of energy mechanisms taking place during methane hydrate production involves the observation and interpretation of phenomena at multiple scales, ranging from the way the hydrate is distributed in sediments at the granular scale to the way the nature of the driving force (e.g., depressurization, thermal stimulation) affect the overall recovery rate. Therefore, the experimental and modeling work will be performed in stages, each of them dealing with a different scale, providing a build-up of knowledge. Intersection of the stages will be the application of the different or combination of driving forces (i.e., the energy driving production). Mathematical models of experimental results will help identify the mechanisms by which each of the driving forces acts efficiently.

The goal of this research is to develop observational and experimental data that can provide a better understanding of the basic mechanisms at work *in a methane hydrate reservoir* that is under production. To this end the recipient shall: (1) gain a thorough physical understanding of underlying phenomena associated with methane hydrate production through unique multi-scale experimentation and associated analyses; and (2) develop one or more mathematical models that account for the observed phenomenon and provide a better understanding that may optimize methane hydrate production methods.

This four year project is organized into seven tasks with a "check point" before task 7, as follows:

Task 1	Research Management Plan	Done	*(brief summary here)*
Task 2	Technology Status Assessment	Done	*(submitted report)*
Task 3	Continuous Literature	In Progress	*(submitted report)*
Task 4	1-D Single Mineral Surface Studies	In progress	*(brief summary here)*
Task 5	2-D Porous Network Studies	In progress	*(brief summary here)*
Task 6	3D Sediment: Experiments using uσ' Cell	Developments under parallel projects	
---------- check point ----------			
Task 7	3D Sediment: Experiments in SPS Cell	Developments under parallel projects	

Highlights of developments during this first year are summarized next, with emphasis on Tasks 4 and 5.

TASK 1.0 RESEARCH MANAGEMENT PLAN

Emphasis during this first year has been placed on effectively starting the project with high productivity. Therefore, the team imvolved 2 Post Docs and a PhD student. More recently, a second PhD student has been incorporated to facilitate the transition as Post Docs leave our institutions. The third PhD student is anticipated to join the team either in the Fall 2007 or Spring 2008.

Four different partners (research groups) participate in this project. The project team consists of:

1. J. Carlos Santamarina and members of his research group at the School of Civil and Env. Engineering of the Georgia Institute of Technology (CEE-GA Tech);
2. Costas Tsouris and members of his research groups at Oak Ridge National Lab. (ORNL) and at Civil and Env. Eng. of Georgia Tech (CEE-GA Tech);
3. Carolyn Ruppel at USGS;
4. Tommy J. Phelps of ORNL.

Santamarina and Tsouris execute the technical objectives of this project, calling upon the other team members to provide input/assistance as needed. The other technical team members were carefully selected for their particular expertise and the high probability of key contributions to the project. The administrative work of the project is performed by Ms. Serelia Woods. She closely tracks the program schedule to ensure all project deliverables are provided to the sponsor. Ms. Serelia Woods prepares the requisite financial reports, handles all invoicing, and ensures compliance with federal accounting laws. Figure 1 presents a flowchart of the project research team management structure.

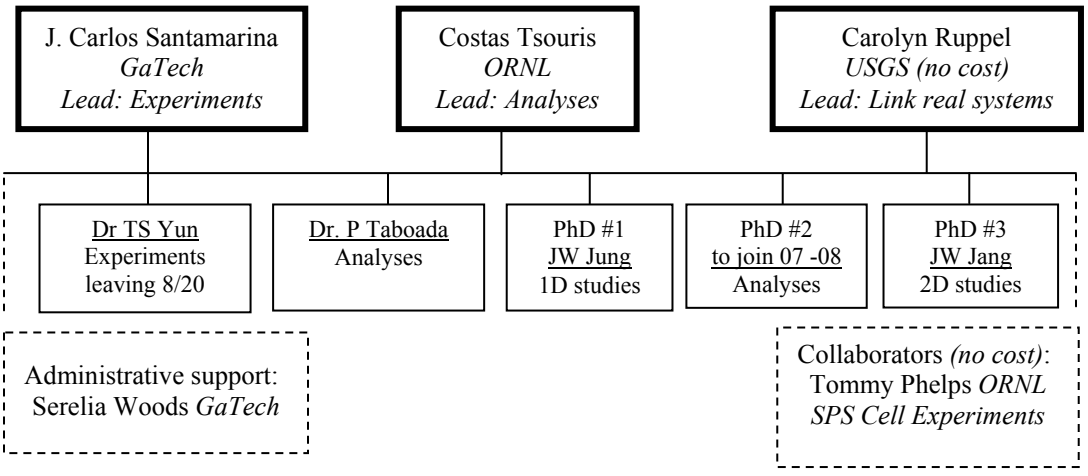

Figure 1 Project research team management structure

TASK 4: 1-D SINGLE MINERAL SURFACE STUDIES

Single-mineral experiments are conducted inside a pressurized chamber designed to allow visualization, stress measurements, mechanical impedance spectroscopy (and Raman spectroscopy if viable). The goal of this task is to obtain experimental information and generate a mathematical model for the dissociation of hydrates associated to mineral surfaces. The experimental work done in this task should improve our understanding of:

1. Intrinsic kinetics of formation and dissociation
2. Effect of mineral surface on kinetics
3. Characterization of the mineral-hydrate-fluid system.

The leading questions that this task attempts to answer include:

- What is the effect of the solid surface on the kinetic behavior of methane hydrates formation and dissociation?
- What are the effects of different potentials (pressure, thermal, chemical and electrical) on stability conditions?
- What are the most relevant phenomena observed during dissociation that may be advantageous for production purposes (e.g., in relation to the different mineralogies, potentials, or self-preservation mechanisms)?
- What are robust yet simple models that can properly capture the observed response?

Subtask 4.1: Single mineral 1-D experiments

Subtask 4.1.1: Design the instrumented pressure vessel

We designed and built a pressure vessel for analysis of a multiple-phase system consisting of contacts and monolayers. We have also developed unprecedented instrumentation for mechanical measurements (stiffness evolution; bonding strength possible), electrical measurements (resistivity evolution, with possible in-plane electrical resistivity tomography), thermal field, and measurements through transparent observation windows (high resolution optical photography with internal illumination). Figures 2, 3 and 4 document some of these developments.

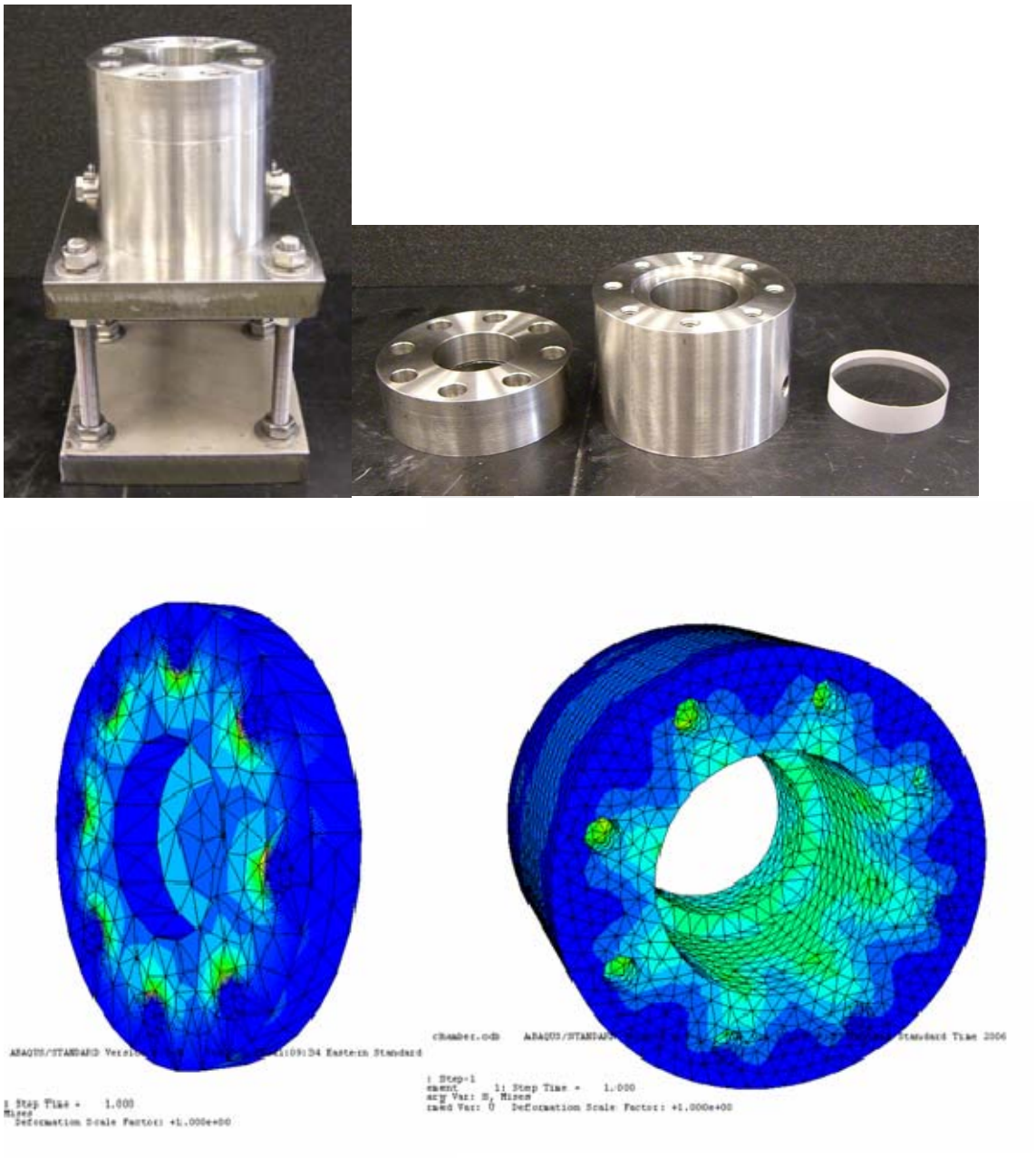

Figure 2: 1D Chamber - Contains 2-inch diameter transparent optical window, accessible ports with electrical feed-through wires and optical feed-through. The cell is designed to withstand 30MPa gas pressure. A comprehensive FEM numerical simulation was conducted to verify design.

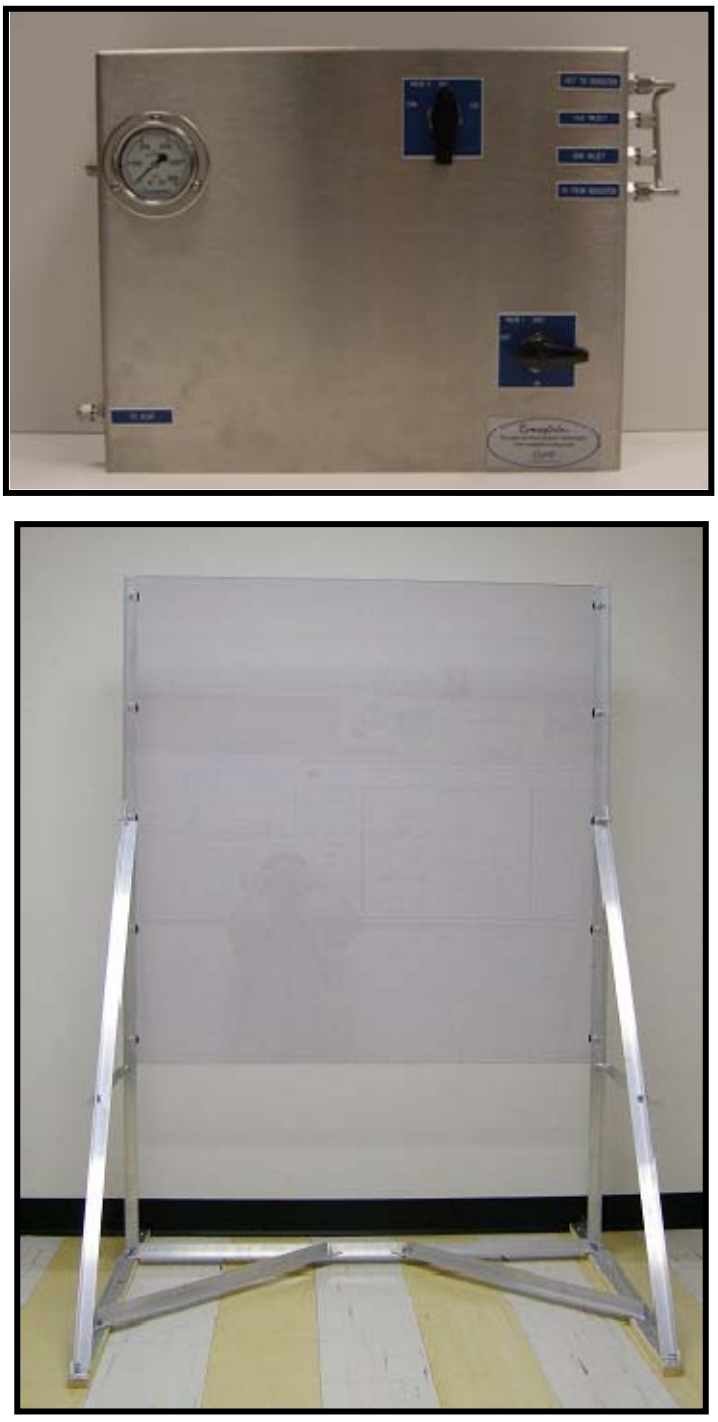

Figure 3: Pressure Control Panel and Protection Shield. This single pressure panel was designed in collaboration with Swagelok to control two gasses (e.g., CO_2 and CH_4) for studies such as production simulation by chemical exchange.

A: Optical feed-through

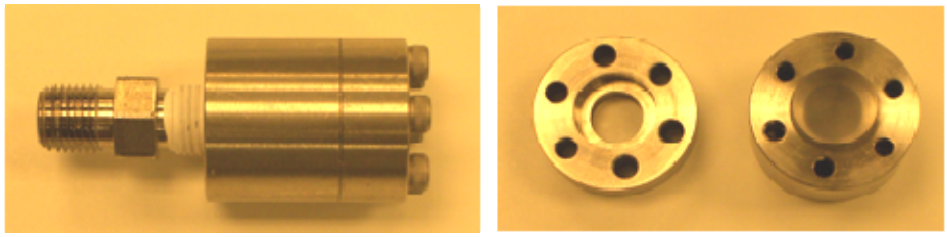

The optical feed-through allows the light illuminated into the pressure chamber when a photo is taken. It is compatible with both 1D and 2D pressure chamber. The figure above shows the polycarbonate disc (dotted section in a left figure), flange and a main body.

B: Sensing table: *Impedance and resistance*

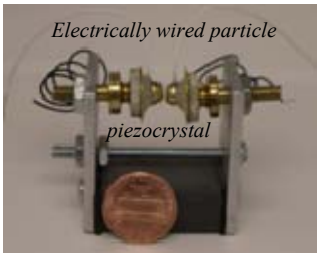

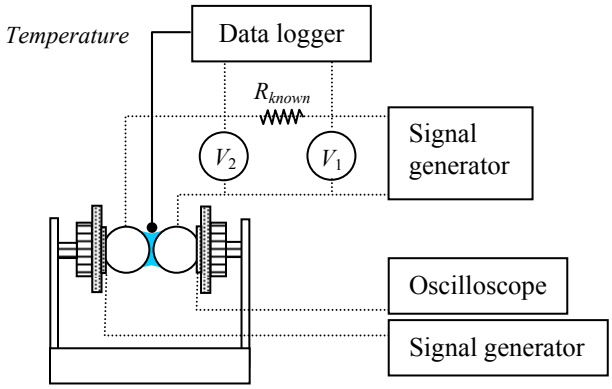

The sensing table houses electrically wired particles which are attached to the piezocrystals. The evolution of electrical conductivity σ_{el} and spectral evolution of impedance change during hydrate formation are measured for various concentrations of saline water, CO_2 / CH_4 gases. Input and output signals travel via electrical feed-through under pressure. Hydrate formation is visually observed through optical window (photos taken before/after hydrate formation are shown later).

C: Electrical Resistance Tomography

It will permit monitoring the evolution of hydrate formation and dissociation in 1D, 2D and 3D systems

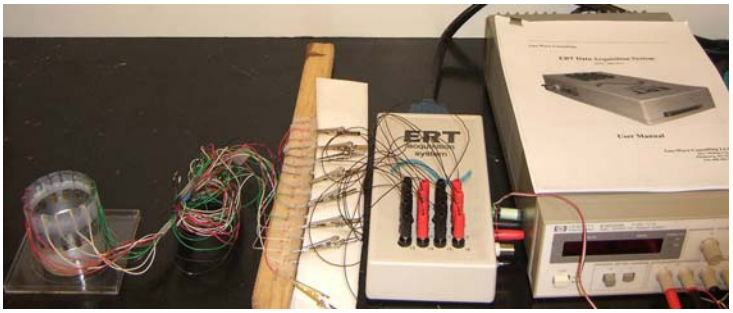

Figure 4: Gadgets. A: Optical feed-through. B: Sensing table - Mechanical and electrical impedance. C: Electrical Resistance Tomograph. D: Pull-out load cell and mechanical actuator (mechanical effects on dissociation & mineral-to-hydrate bonding strength studies).

D: Pull-out load cell and mechanical actuator: Mineral-hydrate bonding strength

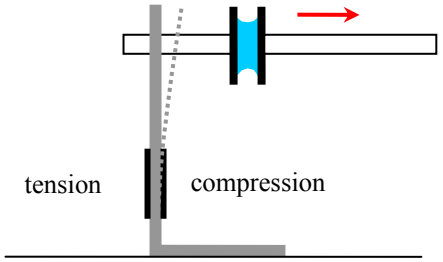

The instrumented angle element is of a full bridge load cell to measure the bonding strength between mineral substrate (quartz, mica, calcite) and hydrate (CO_2 and CH_4). A close up and calibration data follow.

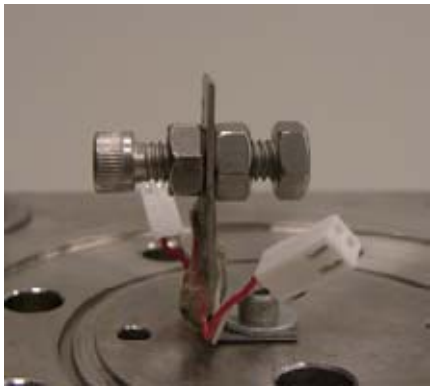

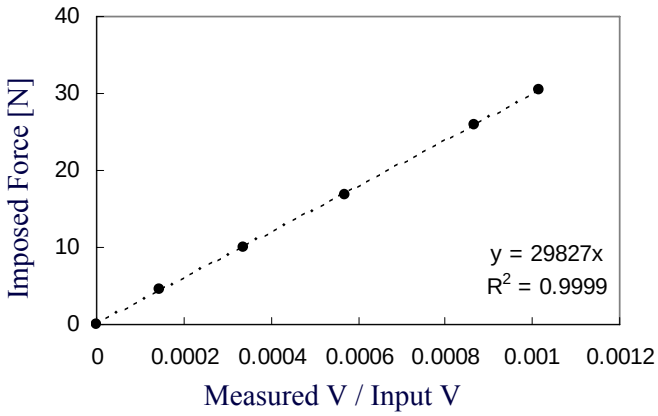

The mechanical actuator is based on the rotation of a driver external to the cell to cause a horizontal pull-out motion of the plate that holds the selected substrate.

Once the substrate is attached to the sensing element and to the driver, a water droplet is placed in between and hydrate formation follows. Then, the pull out test is performed.

Figure 4: Gadgets (continued)

Subtask 4.1.2: Prototype and first set of data

The pressure vessel, instruments and peripheral electronics and control panel designed and built as part of Subtask 4.1.1 are being tested to confirm their capabilities as well as their ability to provide the required data. The vessel has been tested for strength and leaks multiple times. Initial experiments on hydrate formation and properties have been performed to test the proper operation of the instrumentation installed on the vessel.

The preliminary tests conducted so far have involved sequential sets of studies using various pore fluids to simulate fresh to saline water. The electrical resistance and mechanical impedance evolution are measured during CO_2 hydrate formation and dissociation. Details of the test sequence follow:

1. Place the instrumented 2-particle micro-model on the cell base.
2. Add a water droplet between the particles to form a fluid meniscus
3. Place the thermocouple partially touching the meniscus
4. Seal cell and increase gas pressure (current tests: CO_2 at ~ 3.8MPa)
5. Gradually decrease the temperature.
6. Log pressure and temperature every 2 seconds.
7. Once 5^{o}C is reached, close the gas pressure and continue decreasing the temperature to ~ 1^{o}C.
8. A 60kHz signal is used to monitor the evolution of the mechanical impedance of the droplet (this frequency is selected from previous exploratory tests to obtain the maximum change). The output voltage is logged every 2 seconds.
9. Electrical resistance is evaluated using a 50kHz sinusoidal wave to avoid electrode polarization effects. Voltage is logged every 2 seconds.

Results for the first test sequence are summarized in Figure 5 (typical signatures) and Figure 6 (observed trends). *Data in Figure 5 show* the exothermic event as the sign of phase transformation at ~ 50min. The pressure remains constant because of the small volume of hydrate (pressure drop is typically observed when hydrate forms in a close system). Electrical resistance and the amplitude of transmitted mechanical vibrations increase during hydrate formation. The time for changes in temperature and impedances coincide. The transparent water between particles shows a concave meniscus before hydrate formation, but it changes into a white, convex shape bridge after hydrate formation.

The compiled dataset in Figure 6 shows that the electrical conductance before hydrate formation increases with increasing ionic concentration. In all cases, the electrical conductance decreases after hydrate formation, however, it is higher for higher ionic concentration because ion exclusion limits hydrate formation in this "closed system". The vibration amplitude increases after hydrate formation indicating solidification, however, the improvement in mechanical transmissivity diminishes with increasing ionic concentration in the fluid; this corroborates incomplete hydrate formation. In fact, the specimen with 1.3 molarity does not show any hydrate formation under the same pressure and temperature condition (for reference: the seafloor molarity is ~0.54 - green line).

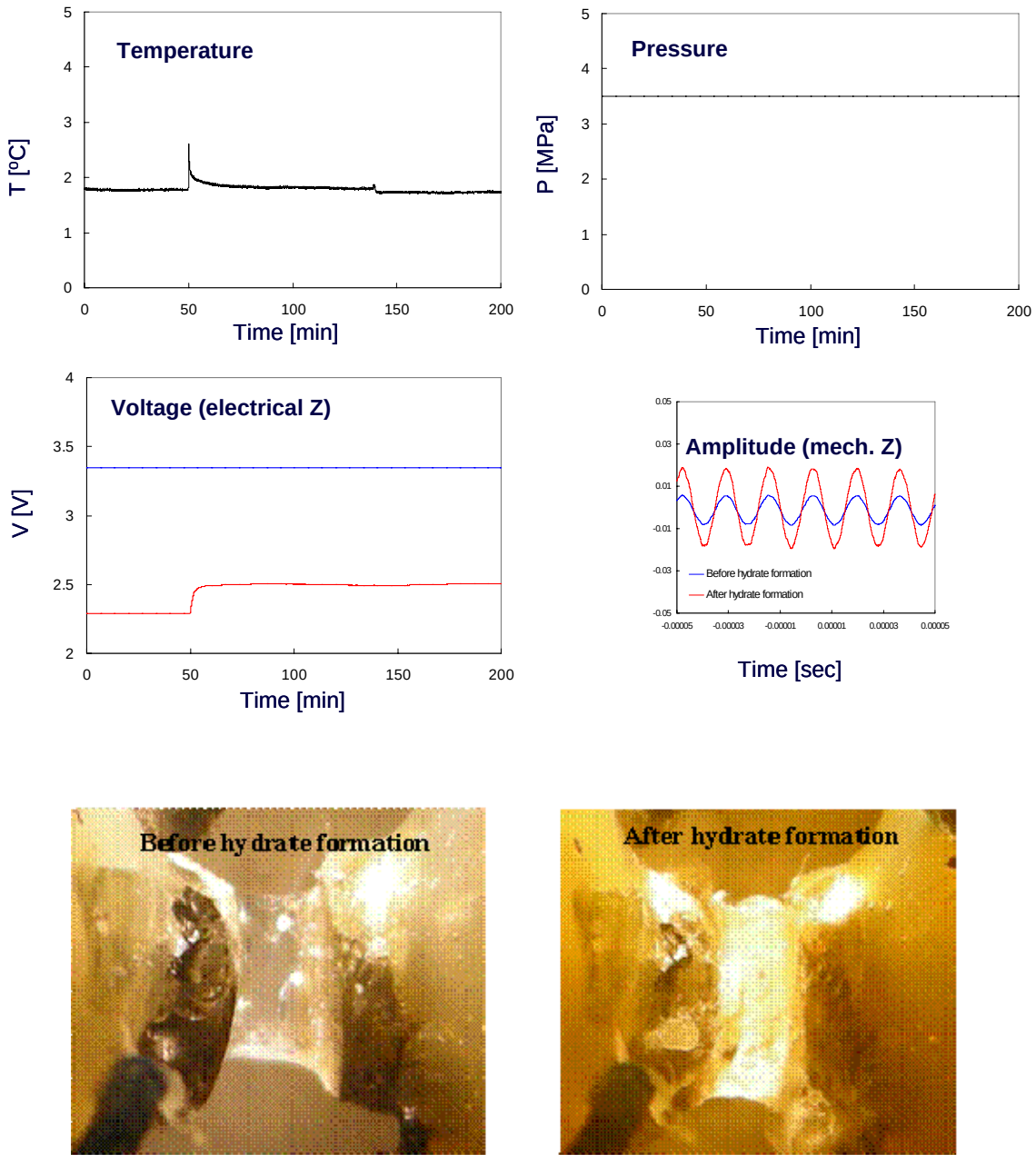

Figure 5: Typical signatures gathered in the contact impedance studies. Data include pressure, temperature, both mechanical and electrical impedance, and digital photography. All data are gathered during hydrate formation and dissociation

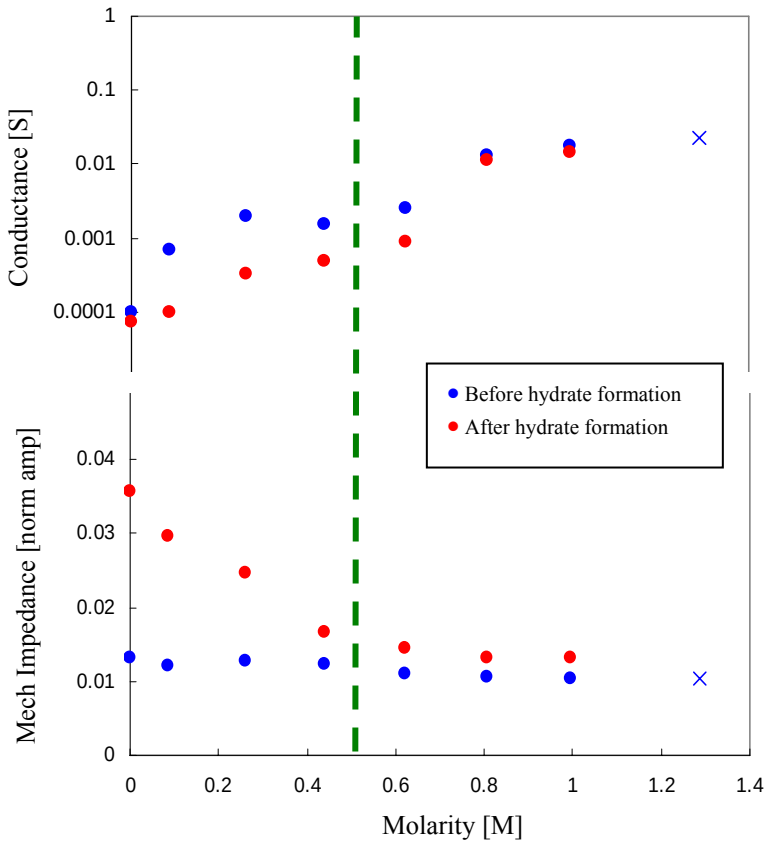

Figure 6: Summary of experimental results (CO_2 hydrate)

Subtask 4.1.3: Complete Single-Mineral 1D Experiments

A test matrix is anticipated for the various combinations of minerals and energy forms to be tested. In general, experiments will be performed at temperatures from 2°C to 8°C, and pressures from 5 to 15 MPa. The water layer tests will involve a fixed water thickness (~1 mm) on the selected mineral substrate and the vessel will be pressurized with methane gas (Figure 7). Calcite, quartz, muscovite, and feldspar will be used for the experiments because of their similarities to materials encountered in hydrate-bearing sediments. Gas hydrate will be allowed to form at the interface of the water/gas film, and it will be characterized via the application of the multiple measurement techniques developed above. A tentative test matrix for Task 4 follows.

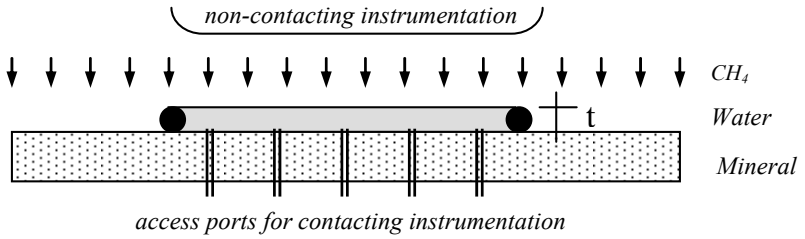

Figure 7 1D tests. Experimental study at the scale of the mineral-water-gas interface.

Tentative Test Matrix - 1D studies

Test #	Production Energy	Substrate	Pore fluid
1	*Depressurization*	Muscovite	de-ionized water
2			seawater
3		Calcite	de-ionized water
4			seawater
5		Glass	de-ionized water
6			seawater
7	*Heating*	Muscovite	de-ionized water
8			seawater
9		Calcite	de-ionized water
10			seawater
11		Glass	de-ionized water
12			seawater
13	*Chemical*	Muscovite	de-ionized water
14			seawater
15		Calcite	de-ionized water
16			seawater
17		Glass	de-ionized water
18			seawater
19	*Electromagnetic*	Muscovite	de-ionized water
20			seawater
21		Calcite	de-ionized water
22			seawater
23		Glass	de-ionized water
24			seawater

Notes

- These tests will be the simplest and fastest to implement (as compared to 2D and 3D studies). Therefore, an extensive experimental study is planned for this Task.
- Expected duration per test: 3 days (additional time required for post-processing).
- Substrates are selected for the wide range of interfacial energies with water, crystalline-amorphous nature, and ability to create planar surface (Muscovite θ= 17º, Calcite θ= 49º, Glass θ= 51º).
- CO_2 is a clear candidate for chemical-driven production, given its chemical advantages and environmental needs (this also provides a link to Batelle's project). Injection in gaseous form will be attempted in view of latter flooding tests.
- Most tests involve coupled energy forms, e.g., shift in P-T stability boundary under chemical exchange or EM excitation
- Experiments beyond core test matrix (e.g., with other gadgets developed above) will be run as needed to complete datasets and validate models (e.g., different concentration of NaCl solution, alternative chemicals, etc)

Subtask 4.2: Intrinsic kinetic model development

The focus of this subtask involved the development of a kinetic model for the dissociation of a gas hydrate film, simulating kinetic experimental studies (see Figure 7). No confinement effects were involved in this part, and the purpose of the model development and analysis was to combine thermodynamics and kinetics in order to describe hydrate dissociation in a simple geometry. After model validation with experimental data, this model can be used for more complicated situations, such as hydrate dissociation in sediments.

Dissociation of a hydrate film: modeling. The following assumptions were made during the formulation of the model:

- The temperature and pressure are uniform inside the system.
- The walls of the pressurized chamber constitute the boundaries of the system.
- The solid and liquid phases are incompressible.
- There are four species present in the system: water, methane, variable amounts of a second gas, and sodium chloride.
- There is no sodium chloride in the solid and gas phases.
- The amount of water transferred to the gas phase is negligible.
- The composition of the solid remains unchanged during dissociation.
- Uniform dissociation takes place.

The model consisted of sixteen ordinary differential and algebraic equations that had to be solved simultaneously via the application of numerical methods. The equations consisted of component mass balances, a global mass balance, an energy balance, a mechanical energy balance on the discharge valve of the pressurized chamber, a hydrate dissociation kinetic expression, gas-liquid equilibrium expressions, gas equation of state, and algebraic expressions for physicochemical properties of all the substances. Four representative equations are presented below as an illustration of the level of complexity of the model.

Equation (1) presents the mass balance for the guest gas molecule (methane):

$$\frac{d}{dt}\left[x_{guest}L + y_{guest}V\right] = -y_{guest}\dot{n}_e + \frac{1}{n_H + 1}\frac{dS}{dt} \quad \equiv \left[\frac{mol}{s}\right] \qquad (1)$$

where t is time; x_{guest} and y_{guest} are the molar fractions of the guest molecule in the liquid and gas phases; L and V are the amounts of moles of the liquid and gas phases; $\check{n}_e$ is the rate of gas removal from the pressurized chamber during dissociation, n_H is the hydration number; and dS/dt is the intrinsic rate of hydrate dissociation. Similar mass balance equations were written for the second gas and water, along with a global mass balance equation.

Equations (2) and (3) represent the energy balance and the mechanical energy balance, respectively:

$$\frac{d}{dt}\left[Su_S + Lu_L + Vu_V + M_{chamber}u_{chamber}\right] = -\dot{n}_e h_e + \dot{Q} \equiv \left[\frac{J}{s}\right] \quad (2)$$

$$\dot{n}_e = C_a A_O \left(P - P_{atm}\right)\left[\frac{M\gamma}{1000\,RT}\left(\frac{2}{\gamma+1}\right)^{(\gamma+1)/(\gamma-1)}\right]^{1/2} \equiv \left[\frac{mol}{s}\right] \quad (3)$$

where u_S, u_L and u_V are the internal energy of the different phases; $M_{chamber}$ and $u_{chamber}$ are the mass and the internal energy of the chamber walls, respectively; h_e is the enthalpy of the exiting gas; Q is the rate of heat transferred to/from the chamber; C_a and A_0 are the discharge coefficient and area of the gas-exhaust valve of the pressurized chamber, respectively; P and P_{atm} correspond to the internal pressure and the external pressure, respectively; M corresponds to the molecular weight of the gas; and γ corresponds to the adiabatic expansion coefficient for the gas.

The kinetic expression depends on the driving force responsible for hydrate dissociation. In the present report, combined depressurization–thermal stimulation will be used to present the outcomes of the model. In this case, the following dissociation kinetic expression was utilized:

$$\frac{dS}{dt} = 3 \cdot k_{dis}\left[2\pi^{1/2}\left(\frac{S}{\hat{\rho}_S}\right)\right]^{2/3} \exp\left(-\frac{E_{act}}{R \cdot T}\right)\left(f - f_{eq}\right) \equiv \left[\frac{mol}{s}\right] \quad (4)$$

where S is the number of moles of hydrate, ρ_S corresponds to the molar density of the hydrate, k_{dis} is the intrinsic dissociation rate at a reference temperature, E_{act} is the activation energy required for dissociation, T is the temperature, and f and f_{eq} correspond to the fugacities of the guest molecule at actual conditions of pressure and temperature and at equilibrium, respectively.

Figures 8 and 9 present the evolution of pressure, temperature, and fraction of hydrate remaining in the pressurized chamber during hydrate dissociation. The model seems to capture well possible phenomena taking place during hydrate dissociation inside the pressurized chamber. It is apparent from Figures 8 and 9 that depressurization and thermal variations during hydrate dissociation occur at two different time scales. While depressurization takes place almost instantaneously, thermal variations are much slower. Furthermore, the rapid loss of gas does not affect the temperature in the system as much as hydrate dissociation does. Significant cooling due to hydrate dissociation slows down the dissociation process significantly.

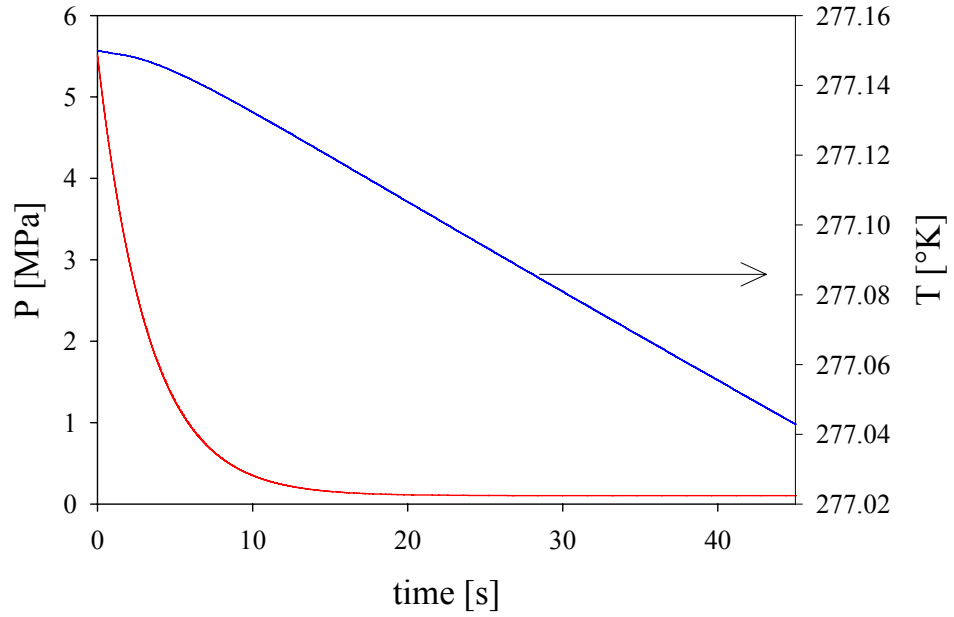

Figure 8. Evolution of pressure and temperature in the pressurized chamber during hydrate dissociation.

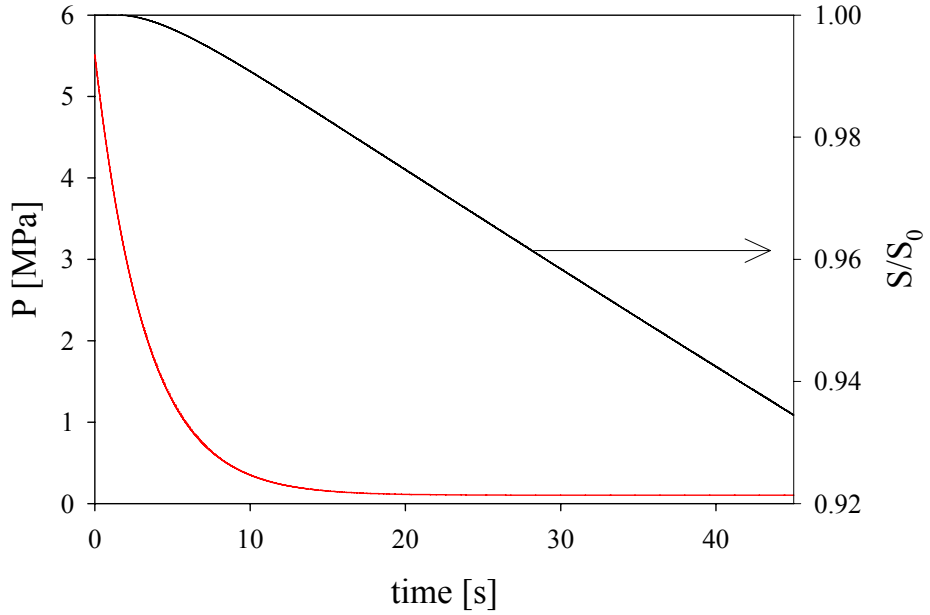

Figure 9. Evolution of pressure and hydrate remaining in the pressurized chamber during dissociation.

Investigation of the suitability of the current thermodynamic model for the description of hydrates in sediments. A thorough literature review on the development and improvements to the current hydrates thermodynamic model was performed to identify elements in the analysis that can be adopted to describe hydrates in sediments. The first conclusion from the literature review was that the description of hydrate equilibrium in both settings (bulk solutions and sediments) could be improved with a m*ore accurate*

description of gas molecule – hydrate cage interactions to improve prediction of cage occupancy and gas content of the hydrate phase. An extended version of the Kihara potential with inclusion of three layers of hydrate lattice has been adapted from the literature, and will be included in the thermodynamic model. A numerical integration method will be used to calculate the energy-interaction parameters required for the description of gas-molecule occupancy of hydrate cages at a constant temperature.

It was also concluded that *a definition of a different standard state for chemical potential of water is necessary to minimize the utilization of empirical expressions*. The most appropriate choice for the standard state for the calculation of the chemical potential of water in the hydrate phase is the reference state (i.e., liquid water at atmospheric pressure and melting point). The chemical potential for water at the reference state will replace the standard state based on the empty hydrate lattice in the model under development. Expressions for the chemical potential change with respect to the reference state are under development. The primary variables of choice are pressure and temperature.

Finally, any adaptation of current thermodynamic models for their application to hydrates in sediments must include the c*onsideration of confinement effects in the overall thermodynamic equilibrium.* The scarce literature available on hydrate equilibrium in porous media suggests the inclusion of a capillary pressure term in the calculation of the chemical potential of water in the hydrate phase to account for the fact that hydrate equilibrium takes place inside confined spaces. Although this approach may work as a first approximation, it neglects other phenomena linked to confinement. The necessity to include the effects of confinement in the criteria for equilibrium: thermal, mechanical, and chemical prompted further literature research on processes analogous to hydrate formation in sediments.

Investigation of analogies between hydrate equilibrium and the thermodynamics of frost damage in soils. Published work on frost damage to porous solids has focused on mechanical equilibrium criteria for the description of growth of ice crystals inside porous media. Unfortunately, the work performed on frost damage in soils is mostly qualitative, and no model describing the solid-liquid equilibrium of water in soils has been developed so far. However, the analysis of the occurrence of ice in soils and the assumption that ice and solid hydrate are analogous crystalline structures, lead us to conclude that two distinct phenomena have to be included in the thermodynamic model under development: (1) capillary effects due to differences of wetting properties of the distinct phases present; and (2) stress imparted by the soil grains on the hydrate solid. Both capillary effects and stress will define the effective pressure of each of the phases—gas, liquid, and solid—inside the porous medium.

0TASK 5: 2-D POROUS NETWORK STUDIES

The study of formation and dissociation of hydrates in porous networks intends to provide insight into emergent phenomena that do not develop in the 1-D mineral surface system, and to introduce transport effects on hydrate dissociation in a controlled manner. The experimental work done in this task should improve our understanding of:

1. The effect of constrained pore geometry
2. Bubble formation and conduction properties
3. Mass transport in porous networks

The leading questions that this task will attempt to answer include:

- Which are the phenomena that deviate destabilization from a homogenous convex process (self-preservation in porous networks, evolution of percolating paths, fingering, capillaries and gas migration)?
- How does dissociation evolve in relation to pore size variability and connectivity, and what are the implications from the point of view of gas recovery? And related implications for modeling?
- Which are the optimal production strategies for low-hydrate concentration in the pore space (S_{hyd}<30%) vs. high hydrate concentration (S_{hyd}>60%).
- How do the different potentials (pressure, thermal, chemical and electrical) affect the evolution of dissolution in porous networks?
- What kind of robust models can one use to properly capture the observed response, with emphasis on gas recovery?

Subtask 5.1: 2-D porous matrix experimental studies

Subtask 5.1.1: Design the instrumented pressure vessel

We have already designed and built the cell that will house the 2D gadets. Based on the experienced gain with the 1D cell and the versatility of this design, we developed the chamber for the 2D cell following a similar configuration, but with a more extensive set of feed throughs, ports and see-through sapphire end windows. The optical window is independently housed within the flange. Two window-flange unit were built, so that the chamber can be operated with windows on both top and bottom ends to attain special test configurations (e.g., to radiate with microwaves); alternatively, a metal bottom plate with additional ports can be used. Figure 10 shows the cell and the numerical verification of different components. The chamber has already been pressure-tested.

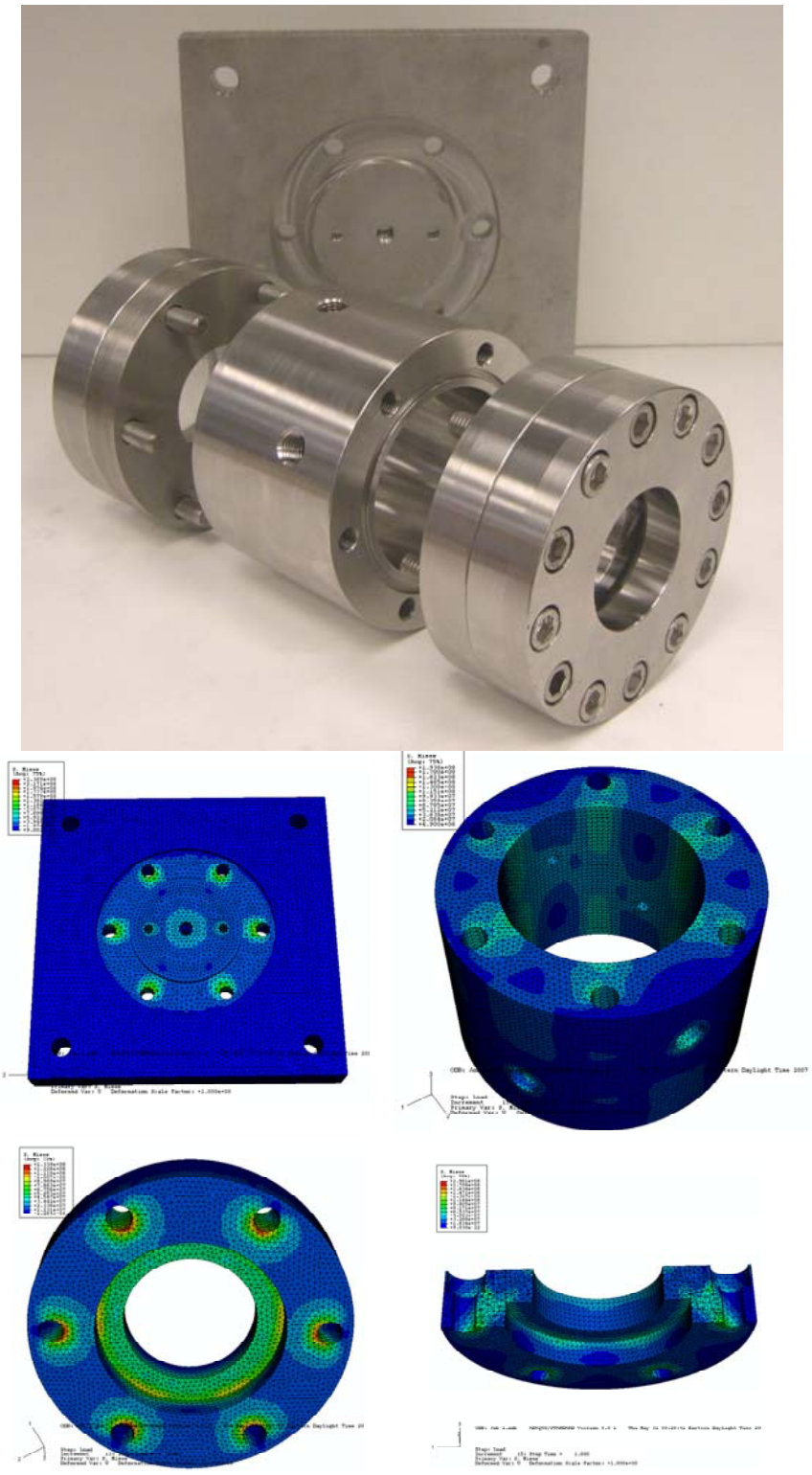

Figure 10: 2D Chamber - It can be operated with either one or two 2-inch ID sapphire windows. It contains 6 accessible ports with electrical feed-through wires and optical feed-through. The cell is designed to withstand 30MPa gas pressure. A comprehensive FEM numerical simulation was conducted to verify the design of all components.

The main gadget is the three-layer glass-particles-glass system designed for the study of multiple-phase conditions in porous networks. The monolayer of granular material (controlled mineralogy) rests in the presence of water, of various compositions, gas and hydrate. The prototype currently being designed and pre-tested is shown in Figure 11. The porous network is placed inside the chamber (Figure 10) where it is subjected to controlled temperature, pressure, chemistry and external fields as needed.

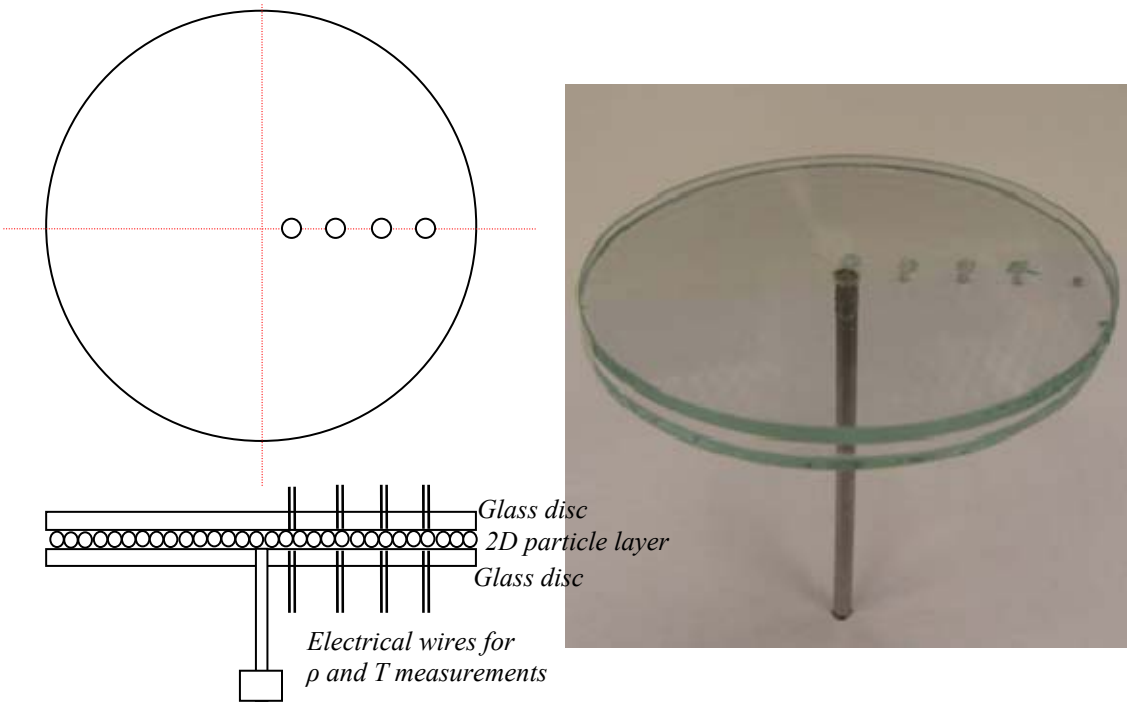

Figure 11: Granular monolayer system for 2D studies - Prototype. Instrumentation ports can be seen in the glass substrates. Instrumentation will include multiple thermocouples, electrodes, and high resolution digital images.

The instrumentation under development includes electrical measurements (resistivity evolution, with possible in-plane electrical resistivity tomography), thermocouples for thermal field assessment, measurements through transparent observation window using high resolution digital photography to obtain images of phase evolution, gas/water front evolution and displacement.

After hydrate formation within the 2D monolayer, dissociation will be initiated and produced methane will be extracted from the center simulating a production well. The radial propagation of the dissociation front will be continuously monitored. We will explore different sensor spacing and geometry to obtain optimal data for inversion/modeling purposes.

Subtask 5.1.2: Prototype and first set of data

The pressurized cell and monolayer gadget will be first tested for its performance in terms of data acquisition and control of experimental conditions. This preliminary study is currently in progress and we plan to complete it during the early part of the summer.

Subtask 5.1.3: Complete 2D experiments and data analysis

A tentative test matrix is being designed to account for the various combinations of minerals, fluids, and energy forms to be tested and conduct these tests. It is anticipated that experiments will be performed at temperatures in the range of 2°C to 8°C, and pressures in the range of 5 MPa to 15 MPa. Methane gas and low-concentration water will be used at this stage to form and dissociate methane hydrates in the porous network.

Tentative Test matrix

Test #	Production Energy	Substrate	Target Hydrate Concentration
1	*Selection 1*	Carbonate sand	S_{hyd}=20%
2			S_{hyd}=80%
3		Quartzitic sand	S_{hyd}=20%
4			S_{hyd}=80%
5		Glass beads	S_{hyd}=20%
6			S_{hyd}=80%
7	*Selection 2*	Carbonate sand	S_{hyd}=20%
8			S_{hyd}=80%
9		Quartzitic sand	S_{hyd}=20%
10			S_{hyd}=80%
11		Glass beads	S_{hyd}=20%
12			S_{hyd}=80%
13	*Selection 3*	Carbonate sand	S_{hyd}=20%
14			S_{hyd}=80%
15		Quartzitic sand	S_{hyd}=20%
16			S_{hyd}=80%
17		Glass beads	S_{hyd}=20%
18			S_{hyd}=80%

Notes

- *Hydrate saturation in the pore space*. The goal is to cover two end-member scenarios which are common field situations as well: disseminated (typically less than 20% - interconnected porosity and high pore fluid conductivity) and high-concentration formations (~ 80% - no percolating paths and the pore fluid conductivity is very low or null). The development of methodologies to attain homogeneous "target saturations" consistently is an important early challenge in this task.
- These tests are more time consuming than those in Task 4 (Expected duration per test: 7 days - additional time required for post-processing). Therefore, test details, such as the selection of coupled energy excitation modes, will be optimized after results from Task 4 are obtained.

- Mineralogy is selected to be complementary to materials tested in Task 4. Glass beads provide a simple geometry for pore-scale modeling.
- It is anticipated that a single pore fluid will be tested in the core sequence for this task, with emphasis on low concentration (this remains a closed system for related time scales). Complementary studies will be conducted with a seawater analogue.
- Experiments beyond the core test matrix will be run as needed to complete datasets and validate models (e.g., different concentration of NaCl solution, alternative chemicals, etc)

Subtask 5.2: 2-D porous matrix model development

The next stage of the project involves the development of a coupled thermodynamic and transport model for hydrate dissociation in sediments. Steps towards the completion of this task have been initiated, as detailed below.

Fundamental thermodynamics analysis: definition of system and establishment of equilibrium criteria. A thorough review of fundamental thermodynamic concepts and methods was used in the definition of a system and equilibrium criteria. Figure 12 presents a schematic of the system in use for the development of the thermodynamic model for hydrate equilibrium in sediments.

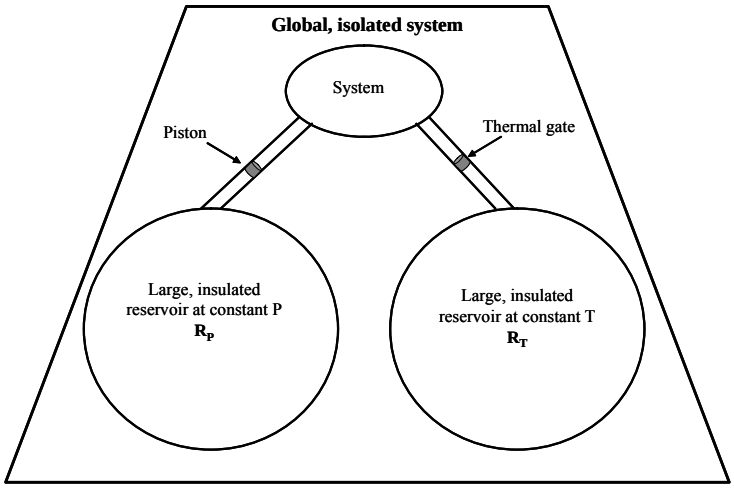

Figure 12. Schematic of the system for the thermodynamic model of hydrate equilibrium in sediments.

The global system is isolated and contains the system of interest and two large reservoirs. A large, insulated pressure reservoir actuates on the system through an adiabatic, impermeable piston; and it is maintained at a constant pressure equivalent to the hydrostatic pressure. A large, insulated thermal reservoir actuates on the system through a rigid, impermeable thermal gate; ant it is maintained at a constant temperature dictated by the geothermic gradient. Since the global system is isolated, global thermodynamic variables like internal energy, entropy, volume and mass will not change, allowing us to minimize energy or maximize entropy of the system of interest to determine conditions for equilibrium. So far, one equilibrium condition has been mathematically established:

(1) equal temperature in all phases (subsystems). The conditions for mechanical and chemical equilibrium are not straightforward for the system of interest.

The system of interest is complex, non-homogenous, and possesses multiple components (e.g., water, methane, and sodium chloride in the simplest scenario). There can be one, two, or even three different phases present in a given state. One or more phases may be highly dispersed as small particles and/or gas cavities. Furthermore, the likelihood of the formation of a new phase and the state of dispersion of the newly formed phase will be determined by the interstitial space in the sediment and the chemical potential of the different species. Discussions about the problem with Prof. John M. Prausnitz (University of California – Berkeley) lead to the conclusion that an innovative approach to this problem is needed.

Nanothermodynamics: equilibrium of dispersed systems. Nanothermodynamics, an emerging field in thermodynamics, allows for the introduction of one additional thermodynamic potential besides pressure, temperature, and chemical potential, which accounts for the fact that phases/subsystems in a macroscopic system may be highly dispersed. The new potential allows for the automatic inclusion of surface effects (i.e., capillary and stress effects in classical thermodynamics) in a simple and natural manner. A thorough review of the literature on nanothermodynamics was performed during the last part of this quarter in order to apply this new theoretical tool to the equilibrium of gas hydrate in sediments.

The system of interest described in section 2 is now considered a complex system composed of an ensemble of subsystems, each of which may be an individual hydrate particle or a gas cavity. The fundamental thermodynamic equation for each subsystem has been modified to account for the grade of dispersion as follows:

$$dU = TdS - PdV + \sum_i \mu_i dN_i + \varepsilon d\eta \qquad (5)$$

where ε corresponds to the new thermodynamic potential accounting for the work involved in creating a small, dispersed subsystem, and η is a measure of the degree of dispersion.

Currently, we are developing the statistical mechanical-based model for the new thermodynamic potential based on the statistical mechanical model already available for gas hydrates. Once this task is completed, the macroscopic, system-wide thermodynamic model and the nanothermodynamic model will be combined for the final description of the equilibrium problem.

Literature reports on the application of nanothermodynamics are quite scarce, and most of them focus on the formation of single-component, vapor bubbles in liquid or the formation of single-component, liquid cavities in bulk vapor. Both problems have been thoroughly studied to help us apply the same procedure to the treatment of gas hydrates in the coming second period of this project.